Interaction Dynamics Characteristics of Detonation Waves with Coolant Flow in a Hydrogen Fuelled Detonation Chamber

Li Jianzhong [1*], *Yuan Li* [2], *Wang Jiahua* [1]

1. Jiangsu Province Key Laboratory of Aerospace Power System,
Nanjing University of Aeronautics and Astronautics, Nanjing 210016, P. R. China
2. School of National Defense Engineering, PLA University of Science and Technology,
Nanjing 210007, P. R. China

(Received 23 March 2016; revised 6 October 2016; accepted 29 October 2016)

Abstract: To analyze the dynamic interaction between detonation waves and coolant flow in a hydrogen fuelled detonation chamber, a hydrogen fuelled detonation chamber with a cooled liner was designed and a simulation model was established. An explicit high-resolution total variation diminishing (TVD) scheme was developed to solve the two-dimensional Euler equations implemented with an augmented reduced mechanism of the hydrogen/air mixture. A point-implicit method was used to solve the numerical stiffness of the chemical reaction source term. The interaction between detonative was and coolant flow were presented. The interaction dynamics between detonation waves and coolant flow in a detonation chamber were investigated. The results indicated that there were some negative interaction effects between detonation waves and coolant flow.

Key words: pulse detonation engine; detonation wave; augmented reduced mechanism; numerical simulation

CLC number: V235.22 **Document code**: A **Article ID**: 1005-1120(2016)06-0687-09

0 Introduction

Pulse detonation engines (PDE) represent a new propulsion system concept that utilizes repetitive detonation combustion to produce thrust or power[1-4]. Compared with a gas turbine engine, PDE has two primary advantages: The capability to operate under unsteady flow and high thermodynamic efficiency with detonation combustion[5-7]. A reduced hardware parts, together with a decrease in pumping requirements, leads to both cost and weight benefits over a conventional propulsion system, which are potential advantages of the PDE. Therefore, PDEs have received increasing attentions in the past decade as a potential new propulsion source for all types of flight vehicles[8]. For a PDE operating at a high frequency, the resulting high gas temperature and pressure fluctuation distributions generated with repetitive detonation combustion are detrimental to the detonation chamber liner material. Therefore, an advanced cooling technology must be used to protect the detonation chamber liner[9-10]. Various techniques, including film cooling, aspiration cooling, and thermal barrier coating, have been successfully used in steady constant pressure combustors to for many years increase the durability of hot components, such as turbine blades and combustor liners[11-18]. Using the national combustion code (NCC) to gain an understanding of the effectiveness of different cooling schemes for a combustion chamber subject to cyclic detonations, several cooling schemes (film cooling, zoned-injection) were studied[19-20]. Based on ejec-

* Corresponding author, E-mail address: ljzh0629@nuaa.edu.cn.

How to cite this article: Li Jianzhong, Yuan Li, Wang Jiahua: Interaction dynamics characteristics of detonation waves with coolant flow in a hydrogen fuelled detonation chamber[J]. Trans. Nanjing Univ. Aero. Astro., 2016, 33(6):687-695.
http://dx.doi.org/10.16356/j.1005-1120.2016.06.687

tor-pumping principles, an alternative, non intrusive cooling scheme was studied with the national combustion code (NCC). The heat flux at the PDC walls was reduced by 20%—30% for the ejector-cooled liner. The heat-flux of several different cooling schemes were compared. Reducing The peak heat flux and the average heat-flux passing by the combustor walls were reduced by film cooling. The average (plateau) heat flux survives a much longer time than the peak heat flux. Therefore, an optimal cooling scheme design should be performed to reduce the plateau heat flux for the combustor liner. Based on the cooling technology of gas turbine engine, film cooling could reduce the baseline value of the time-averaged plateau heat flux by 64%[21]. A film cooled liner were conducted on the constant volume combustion cycle engine (CVCCE) in Cell 21 of the Research Combustion Laboratories, NASA Glenn Research Center[22]. The post-detonation ("plateau") heat-flux at the exit of the cooling-hole was reduced by 45%—50% and further a 25%—30% reduction at 2.5 mm downstream of the cooling-hole was achieved. Since the range of flow velocities in a detonation chamber is very large and unsteady, it is difficult to analytically determine the contribution to the heat load from the purging, filling, detonating, and blow down portions of the cycle[23-24]. The effects of the operating parameters on the detonation chamber heat load were examined, especially the equivalence ratio and the cycle frequency. The temperature fluctuation and depth of penetration were found to decrease with an increasing detonation operating frequency[25].

Past research focused on the thermal fatigue and material of the detonation chamber liner. In contrast, the interaction between detonation waves and coolant flow has been neglected. This effect could lead to a decrease of the cooling effectiveness and changes in the detonation wave properties. In this paper, the interaction dynamics between the detonation waves with coolant flow in a hydrogen fuelled detonation chamber were investigated and the cooling efficiency of the film cooled liner chamber was neglected. To solve the two-dimensional Euler equations implemented with the skeletal and reduced chemical reaction kinetics of hydrogen/air mixture, an explicit total variation diminishing (TVD) scheme and a point-implicit mechod were utilized. Many images of the interaction process between detonative waves and coolant flow were presented to investigate the interaction between the detonative waves and coolant flow.

1 Physical and Computational Model

The optimal geometry of the cooling models and mass-flow rate of the coolant should provide adequate heat-removal from the chamber liner. And the coolant film should have a sufficient momentum to survive the passage of the detonation wave. An additional criterion for a practical liner is that there should be adequate axial and circumferential film coverage on the liner to prevent hot locations. A cooling geometry of the detonation chamber liner is shown in Fig. 1. By assuming flow symmetry, the computational domains were simplified as 2D regions, as shown in Fig. 2, where the cooling slot width of 2 mm and the coolant mass-flow rate of 3.5% of the detonation chamber mass-flow rate are the same as those in the practical geometry case. The cooling slot was filled with a dilution gas of N_2 at a given initial temperature T_0, pressure p_0, and flow velocity U_0, where the initial state of $p_0 = 0.1$ MPa and $T_0 = 275$ K. The physical domain was filled with a detonable gaseous mixture at a given initial temperature T_0, pressure p_0, and flow velocity U_0, where a stoichiometric hydrogen/oxygen mixture was filled in the physical domain at the initial state of $p_0 = 0.1$ MPa and $T_0 = 500$ K, and the dilution rate of nitrogen is 49%. The ignition source is taken to be a hot location of the burned gas ($p_{ig} = 1.2$ MPa and $T_{ig} = 2\,400$ K) for the direct initiation of the detonation with a minimum initial overdriven effect.

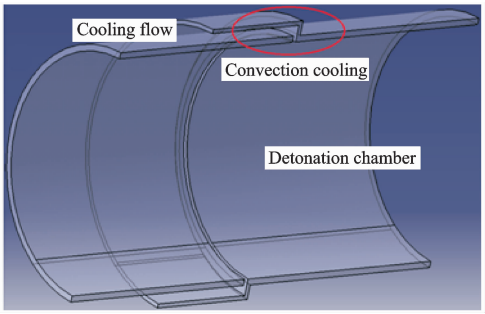

Fig. 1 Feature of the cooling model for a detonation chamber liner

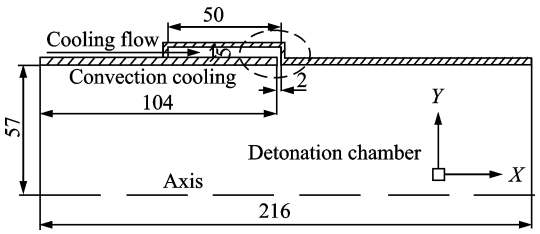

Fig. 2 The simplified computational domains for the practical cooling geometry

2 Governing Equations and Chemical Kinetics

In the dynamic process of detonation propagations, the flow field of interest is symmetry and the effect of viscosity is negligible. Therefore, the governing equations for detonations can be simplified as the 2D reactive Euler equations in Cartesian coordinate system and they can be written as

$$\frac{\partial \boldsymbol{U}}{\partial t}+\frac{\partial \boldsymbol{F}}{\partial x}+\frac{\partial \boldsymbol{G}}{\partial y}+\frac{i}{y}\boldsymbol{S}_{\mathrm{g}}=\boldsymbol{S}_{\mathrm{c}} \tag{1}$$

$$\boldsymbol{U}=\begin{bmatrix}\rho_1\\ \rho_2\\ \vdots\\ \rho_{ns}\\ \rho u\\ \rho v\\ \rho e\end{bmatrix},\ \boldsymbol{F}=\begin{bmatrix}\rho_1 u\\ \rho_2 u\\ \vdots\\ \rho_{ns} u\\ \rho u^2+p\\ \rho uv\\ (\rho e+p)u\end{bmatrix},\ \boldsymbol{G}=\begin{bmatrix}\rho_1 v\\ \rho_2 v\\ \vdots\\ \rho_{ns} v\\ \rho uv\\ \rho v^2+p\\ (\rho e+p)v\end{bmatrix}$$

$$\boldsymbol{S}_{\mathrm{g}}=\begin{bmatrix}\rho_1 v\\ \rho_2 v\\ \vdots\\ \rho_{ns} v\\ \rho uv\\ \rho v^2+p\\ (\rho e+p)v\end{bmatrix},\ \boldsymbol{S}_{\mathrm{c}}=\begin{bmatrix}w_1\\ w_2\\ \vdots\\ w_{n_s}\\ 0\\ 0\\ 0\end{bmatrix} \tag{2}$$

where $\boldsymbol{U}$ is an unknown vector, ρ_i the density of the species $i(i=1,2,\cdots,n_s)$, and ρ the density of mixture. $\boldsymbol{F}$ and $\boldsymbol{G}$ are the convective fluxes, $\boldsymbol{S}_{\mathrm{g}}$ and $\boldsymbol{S}_{\mathrm{c}}$ the geometrical and chemical reaction source terms, respectively, u and v the velocity components in x- and y-directions, respectively, p is the sum of the partial pressure for each species according to Dalton′s law with the ideal gas equation of state, and e the total energy per specific volume. The variables p and e are written as

$$p=\sum_{k=1}^{ns}\frac{\rho_k}{M_k}RT \tag{3}$$

$$e=h-\frac{p}{\rho}+(u^2+v^2)/2 \tag{4}$$

High-resolution explicit TVD schemes were applied to the gas equations. As a characteristic of explicit second-order accurate schemes, while the shock front is narrow, the scheme does not generate spurious oscillations and it would be highly accurate whenever the solution is smooth. In addition, the scheme also overcomes the disadvantage of the slow convergence rate of explicit schemes by auto-dropping off to first-order accurate schemes at the leap point. By solving the 2D Euler equations coupled with the chemistry, a numerical simulation of the transient detonation process induced by the flame for the $H_2/O_2/N_2$ mixture was performed. Using a computer algorithm for the automatic generation of the reduced chemistry, an augmented reduced mechanism, consisting of 11 species (H_2, H, O_2, O, OH, HO_2, H_2O_2, H_2O, N_2, N, NO) and 23 lumped reaction steps, was used for the $H_2/O_2/N_2$ reaction mechanism, as presented in Table 1. A splitting operator method was used to separately treat the aerodynamic process and the chemical process in the detonation simulation[26-27].

The source terms, ω_i, for $i=1,2,\cdots,n_s$, in Eq. (1) are the summation of the net rates of change of species i from all chemical reactions involved, which is written as

$$w_i\equiv\frac{\partial \rho_i}{\partial t}=M_i\sum_{k=1}^{n_r}(v''_{i,k}-v'_{i,k})\times\left[k_{f,k}\prod_{j=1}^{n_s}(X_j)^{v'_{j,k}}-k_{b,k}\prod_{j=1}^{n_s}(X_j)^{v''_{j,k}}\right] \tag{5}$$

where M_k is the molecular weight of species i, n_r the number of chemical reactions being considered in the detonation, $v''_{i,k}$ and $v'_{i,k}$ are the stoichiometric coefficients of the reactants and the products, respectively, for species i in the k th reaction. $k_{f,k}$ is determined by the Arrhenius equation. Table 1 provides the Arrhenius parameters for the hydrogen-oxygen mixture. $k_{b,k}$ is the backward reaction rate constant, given by $k_{b,k} = k_{f,k}/k_{c,k}$, and $k_{c,k}$ is the equilibrium constant for the chemical reaction. X_j is the mole concentration of species j.

The rate constants are listed in the form ($k = AT^n \exp(-E_a/RT)$).

Table 1 $H_2/O_2/N_2$ augmentedus reduced mechanism

No.	Lumped reaction	A	n	E_a
1	$H+O_2+M \Leftrightarrow HO_2+M$	2.800E+18	−0.86	0.0
2	$2H+M \Leftrightarrow H_2+M$	1.000E+18	−1.0	0.0
3	$2H+H_2 \Leftrightarrow 2H_2$	9.000E+16	−0.6	0.0
4	$2H+H_2O \Leftrightarrow H_2+H_2O$	6.000E+19	−1.25	0.0
5	$H+OH+M \Leftrightarrow H_2O+M$	2.200E+22	−2.0	0.0
6	$O+H+M \Leftrightarrow OH+M$	5.000E+17	−1.0	0.0
7	$2O+M \Leftrightarrow O_2+M$	1.200E+17	−1.0	0.0
8	$2OH(+M) \Leftrightarrow H_2O_2(+M)$	7.400E+13	−0.37	0.0
9	$H_2+O_2 = 2OH$	1.700 0E+13	0.0	47 780
10	$OH+H_2 \Leftrightarrow H+H_2O$	2.160E+08	1.51	3 430.0
11	$H+O_2 \Leftrightarrow O+OH$	2.650E+16	−0.671	17 041.0
12	$O+H_2 \Leftrightarrow H+OH$	3.870E+04	2.7	6 260.0
13	$OH+HO_2 \Leftrightarrow O_2+H_2O$	1.450E+13	0.0	−500.0
14	$H+HO_2 \Leftrightarrow 2OH$	0.840E+14	0.0	635.0
15	$O+HO_2 \Leftrightarrow OH+O_2$	2.000E+13	0.0	0.0
16	$2OH \Leftrightarrow O+H_2O$	3.570E+04	2.4	−2 110.0
17	$H+HO_2 \Leftrightarrow O_2+H_2$	4.480E+13	0.0	1 068.0
18	$2HO_2 \Leftrightarrow O_2+H_2O_2$	1.300E+11	0.0	−1 630.0
19	$H+H_2O_2 \Leftrightarrow HO_2+H_2$	1.210E+07	2.0	5 200.0
20	$OH+H_2O_2 \Leftrightarrow HO_2+H_2O$	2.000E+12	0.0	427.0
21	$N+NO \Leftrightarrow N_2+O$	2.700E+13	0.0	355.0
22	$N+O_2 \Leftrightarrow NO+O$	9.000E+09	1.0	6 500.0
23	$N+OH \Leftrightarrow NO+H$	3.360E+13	0.0	385.0

3 Validation of Numerical Methods and Codes

To verify the models and numerical code, a specific case was simulated. The case used to validate the applied chemical reaction model is a planar detonation propagating in a straight tube. The gaseous mixture is stoichiometric hydrogen/oxygen with a 70% nitrogen dilution with initial conditions of $p_0 = 0.1$ MPa and $T_0 = 300$ K. The statistics of the numerical data indicated that the detonation speed is 1 632.4 m/s. The use of shock waves for the study of high-temperature gas reactions was described[28], with particular emphasis on the ignition of the gas mixtures, the transition of combustion to detonation, and the structure of the detonation waves. The statistics of the experimental data indicated that the detonation speed is 1 623 m/s. The corresponding data calculated with the detailed chemical reaction mechanism are 1 619 m/s for the CJ detonation speed. The discrepancy was only 0.828%; hence, the reliability of the present chemical reaction model was well demonstrated.

4 Results and Discussions

Temperature contours versus time in detonation combustor was shown in Fig. 3. Before the time of 0.091 4 ms, the detonation chamber was being inflated. A short cooling film was formed and protect the detonation chamber liner. At the time of 0.103 6 ms, the detonation waves were initiated with high temperature and high pressure zone and the detonation wave propagated with

constant speed. When the detonation waves met with the nitrogen cooling film, they diffracted to be curved waves and destroyed the shape of cooling film. The curved detonation waves transmitted and reflected from the chamber wall (shown in Fig. 4). The complex waves were formed and the cooling film was destroyed into a cooling bubble. At the time of 0.152 7 ms, some detonation waves decreased to be shock waves and transmit into the cooling flow cavity and the lead detonation waves propagated downstream. The detonation waves exhausted out of detonation chamber and the expansion waves were produced and propagated upstream to decrease the pressure of the detonation chamber. Since the pressure of detonation chamber was lower than the cooling flow, the cooling flow was refilled into detonation chamber at the time of 0.248 3 ms. The pressure of detonation chamber fell significently and the difference of pressure increased between the cooling flow and chamber, then, the cooling flow jet would be strengthen and the jet trajectory exhibited liked a mushroom shape, as shown in Fig. 5. The jet penetration depth was increased until the jet trajectory penetrated the cross section of detonation chamber at the time of 0.356 5 ms. The jet cut off the interaction between the wake flame and the fresh detonative mixture. The jet could work as buffer gas to avoid auto-ignition. Mole fraction contours of H_2 and H_2O represents the fresh mixture and high-temperature-burned gas respectively and the isolation function of jet was verified.

The schematic of the monitored spot was shown in Fig. 6. The parameters variation profile as a function of run time of the cavity, gap and detonation chamber were monitored. The parameters of pressure, temperature and axial velocity were gained. The coordinate of the monitored spots was shown in Table. 2.

Parameter profiles versus time at position a_1, a_2, a_3 were shown in Fig. 7, where Fig. 7(a) is pressure, Fig. 7(b) temperature, Fig. 7(c) axial velocity. when a_1 was at the upstream position of cooling flow gap, the pressure of detonation waves would not be affected by the cooling flow.

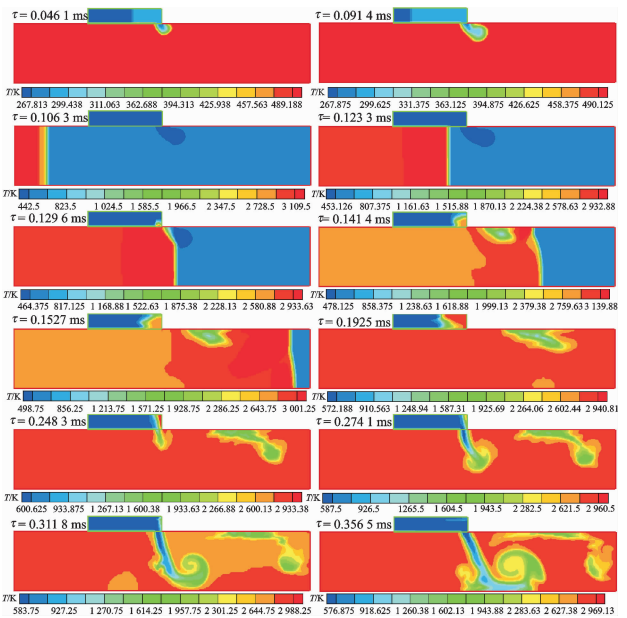

Fig. 3 Temperature contours versus time in detonation combustor

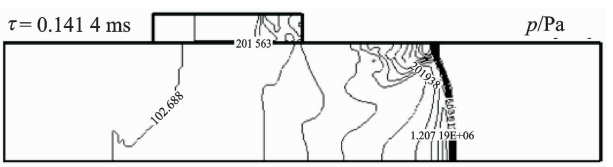

Fig. 4 Pressure contour in detonation chamber

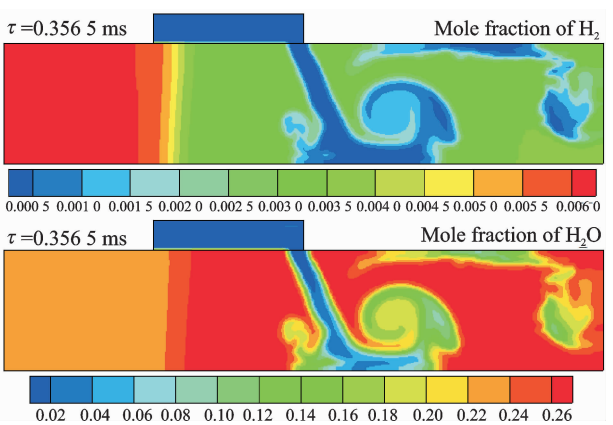

Fig. 5 Mole fraction contours of H_2 and H_2O in detonation chamber

Table 2 The coordinate of the monitored spots

Spot	x	y	Spot	x	y
a_1	92	37	c_1	110	37
a_2	125	30	c_2	120	37
a_3	180	20	c_3	130	37
b_1	60	45	d_1	110	40
b_2	90	45	d_2	120	40
b_3	90	40	d_3	130	40

Because of the effect of the dilution gas of N_2, the pressure and axial velocity of position a_2, which was at the edge of cooling film, were lower than that at position a_1. Before the time of 0.27 ms, the parameters at position a_3 were steady as CJ detonation waves. After the time of 0.27 ms, the cooling jet flow decreased the temperature of chamber quickly and avoided the auto-ignition.

Parameter profiles versus time at position b_1, b_2, b_3 were shown in Fig. 8, where (a) is pressure, (b) temperature, (c) axial velocity. Since the detonation waves decreased ino shock waves and would transmit upstream through the cavity, the pressure oscillation at position b_1 and b_2 were very large. The temperature at position b_1 was affected slightly. Since b_3 and chamber were linked together, the pressure and temperature varied greatly at position b_3. The temperature and axial velocity at position b_2 indicated that the detonation waves brought the high temperature burned gas into the cavity and affected the cooling flow field. After the pressure of chamber decreased, the cooling flow was refilled the chamber and formed into jet flow with high speed and existed for 0.05 ms. The isolation function was ensured by this jet flow which was formed by cooling flow.

Parameter profiles versus time at position c_1, c_2, c_3 were shown in Fig. 9, where Fig. 9(a) pressure, Fig. 9(b) temperature, Fig. 9(c) axial velocity. Because of the effect of the dilution gas of N_2 at position c_1, the pressure, temperature and axial velocity were lower. The detonation waves met the wall and appeared mach reflection so that the spike pressure at position c_2 and c_3 were larger. After the time of 0.15 ms, the temperature at position c_2 and c_3 decreased firstly and then increased, for that the temperature was affected greatly. The detonation wave cut off the cooling flow and would be formed as cooling flow bubble which was shown in the image at the time of 0.141 4 ms and 0.356 5 ms in Fig. 3. When the cooling flow bubble was moving downstream, there was energy and momentum exchange between the cooling flow bubble and the high temperature burned gas so that the detonation

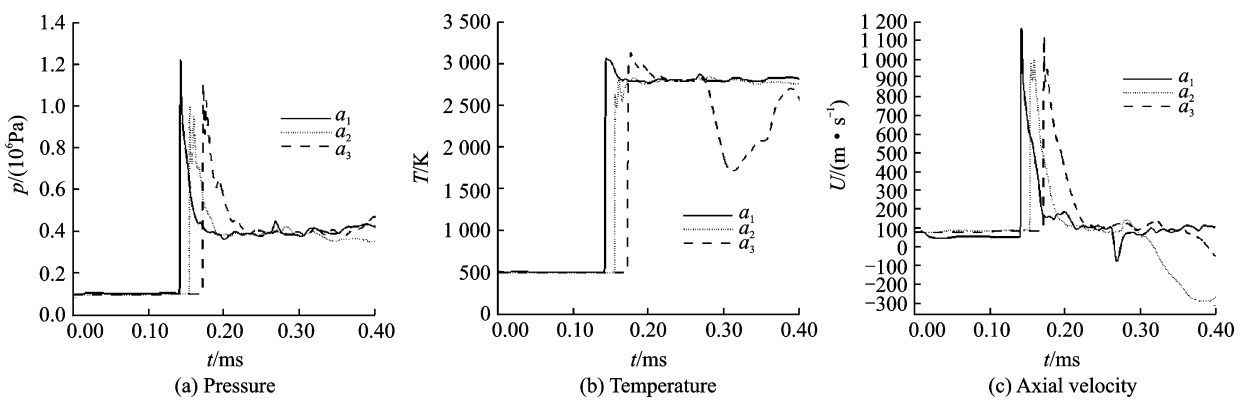

Fig. 7 Parameter profiles versus time at position a_1, a_2, a_3

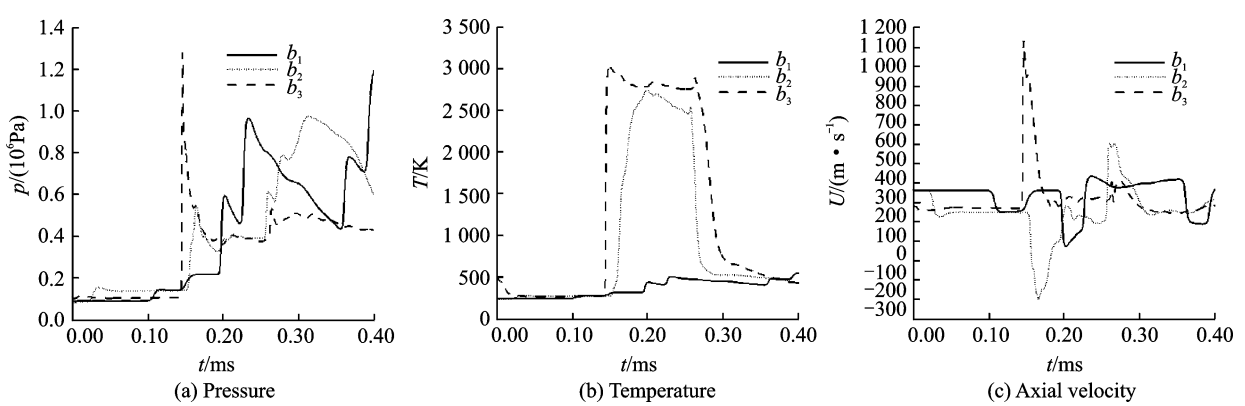

Fig. 8 Parameter profiles versus time at position b_1, b_2, b_3

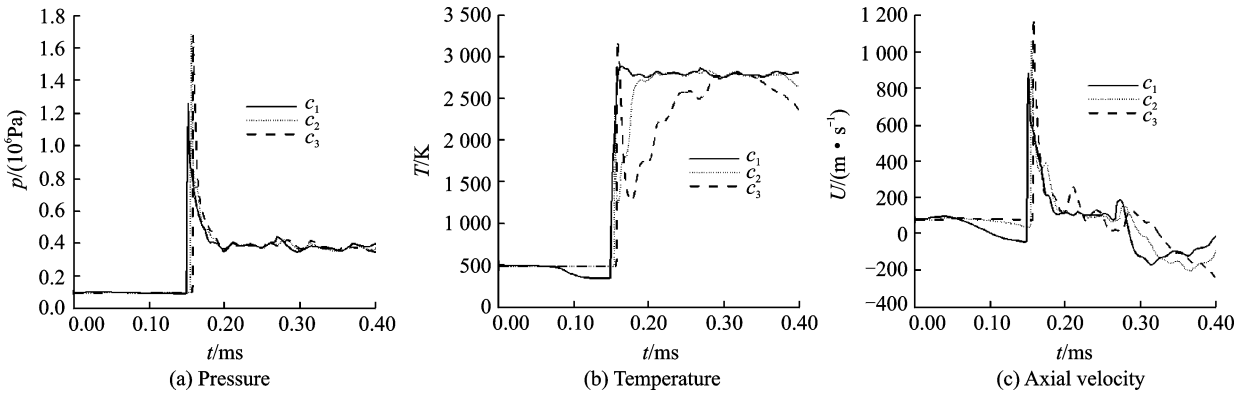

Fig. 9 Parameter profile versus time at position c_1, c_2, c_3

chamber liner would be cooled as a function of thermal protection.

Temperature profiles versus time at position d_1, d_2, d_3 was shown in Fig. 10. The cooling flow gas film could protect and cool the chamber liner. The arrived detonation waves would destroy the shape of cooling flow film and the cooling flow bubble would be formed. The cooling flow bubble moved downstream through the wall of chamber and continued to cool the chamber liner.

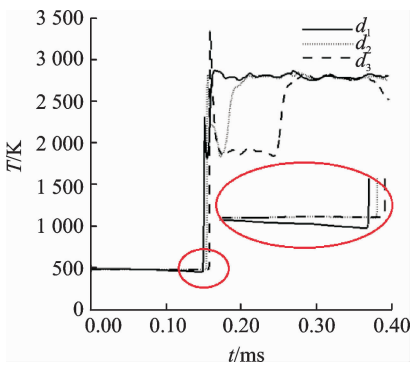

Fig. 10 Temperature profiles versus time at position d_1, d_2, d_3

5 Conclusions

The program of a chemical reaction flow with a $H_2/O_2/N_2$ skeletal and reduced reaction mechanism was developed. The convectional cooling geometry was chosen to cool the detonation chamber liner, and the physical models of the cooling geometry were established. The interaction between the detonation waves and the coolant flow in the detonation chamber was investigated.

(1) The interaction between the coolant flow and detonative waves were presented in images. The planar detonation wave front was changed into the curved detonation wave and the detonation temperature would decrease near the slot for filling a cooling flow. This results would affect detonation propagation in chamber.

(2) When detonation moved out of the chamber, the pressure of detonation chamber fell significantly and the cooling flow jet would be strengthen and the jet trajectory looked like a mushroom cloud. The cooling flow jet could work as buffer gas and avoided auto-ignition.

(3) The detonation wave properties were changed by the effect of coolant flow for the chamber liner and that the detonation wave destroyed the structure of the coolant flow film. The interaction effect and mechanism of the detonation waves and the coolant flow were obtained. When designing a cooling geometry for detonation chamber, the interaction between the detonation waves and the unsteady flow must be considered in detail.

Acknowledgment

This work was supported by the National Natural Science Foundation of China (No. 51476077).

References:

[1] DRISCOLL R, RANDALL S, St GEORGE A, et al. Development and investigation of an air-breathing, pulse detonation engine-crossover system: AIAA 2015-1347[R]. 2015.

[2] BELLO R T, LU F K. Performance model for fully and partially filled pulse detonation engine: AIAA

2015-1352[R]. 2015.

[3] JOSHI D D, LU F K. Unsteady thrust measurement for pulse detonation engines: AIAA 2014-3541[R]. 2014.

[4] CARTER J D, LU F K. Experiences in testing of a large-scale, liquid-fueled, air-breathing, pulse detonation engine: AIAA 2011-6089[R]. 2011.

[5] MASASHI W, MASAYOSHI T, AKIHIRO T, et al. Detonation transition around cylindrical reflector of pulse detonation engine initiator [J]. Journal of Propulsion & Power, 2013, 29(4): 825-831.

[6] WOLANSKI P. Detonative propulsion [J]. Proceedings of the Combustion Institute, 2013, 34(1): 125-158.

[7] MATTISONA D W, OEHLSCHLAEGERA M A, MORRISB C I, et al. Evaluation of pulse detonation engine modeling using laser-based temperature and OH concentration measurements [J]. Proceedings of the Combustion Institute, 2005, 30(2): 2799-2807.

[8] RASHEED A, FURMAN A H, DEAN A J. Experimental investigations of the performance of a multitube pulse detonation turbine system [J]. Journal of Propulsion & Power, 2011, 27(3): 586-596.

[9] ZHU D, FOX D S, MILLER R A. Oxidation and creep-enhanced fatigue of haynes 188 alloy-oxide scale system under simulated pulse detonation engine conditions [J]. Ceramic Engineering and Science Proceedings, 2002, 23(4): 547-553.

[10] ZHU D, FOX D S, MILLER R A, et al. Effect of surface impulsive thermal loads on fatigue behavior of constant volume propulsion engine combustor materials [J]. Surface & Coatings Technology, 2004, 188/189(1): 13-19.

[11] MARTINEZ S R, RICKLICK M A. Benchmarking of computational models for adiabatic film-cooling effectiveness for large spacing compound angle full coverage film cooling arrays: AIAA 2015-2813[R]. 2015.

[12] KUMUD A, BREISACHER K J, GHOSN L J, et al. Numerical and experimental studies of a film cooled pulsed detonation tube: AIAA 2004-3509[R]. 2004.

[13] DANG Xinxian, ZHAO Jianxing, JI Honghu. Effects of primary holes on flow fields of dual swirl combustor [J]. Journal of Nanjing University of Aeronautics & Astronautics, 2008, 40 (1): 26-31. (in Chinese)

[14] HU Haosheng, CAI Wenxiang, ZHAO Jianxing. Numerical study of cold flow field in gas turbine combustor[J]. Journal of Nanjing University of Aeronautics & Astronautics, 2005, 37(6): 704-708. (in Chinese)

[15] LI Jinghua, ZHAO Jianxing, CHANG Haiping. Numerical simulation of gas turbine annular combustor with two-stage swirler[J]. Journal of Nanjing University of Aeronautics & Astronautics, 2007, 39(6): 781-785. (in Chinese)

[16] ZHOU Wenwu, JOHNSON B, HU Hui. An experimental study of momentum-preserving shaped holes for film cooling using psp and PIV: AIAA 2014-0280 [R]. 2014.

[17] KNIPE K, MANERO A, SIDDIQUI S F, et al. Synchrotron XRD measurements of thermal barrier coatings subjected to loads representing operational conditions of rotating gas turbine blades: AIAA 2014-1157[R]. 2014.

[18] ZHU D M, FOX D S, MILLER R A, et al. Effect of surface impulsive thermal loads on fatigue behavior of constant volume propulsion engine combustor materials: NASA TM-2004-213084[R]. 2004.

[19] AJMANI K, BREISACHER K J. Multi-cycle analysis of an ejector-cooled pulse detonation device: AIAA 2004-3915[R]. 2004.

[20] AJMANI K, BREISACHER K J. Qualitative study of cooling methods for a pulse-detonation engine [C]//51st JANNAF Propulsion Meeting. USA: NASA, 2002.

[21] SAMPATH P, MCCALDON V J K. Low emissions technology for small aviation gas turbines: AIAA 2003-2564[R]. 2003.

[22] AJMANI K, BREISACHER K J, GHOSN L J, et al. Numerical and experimental studies of a film cooled pulsed detonation tube: AIAA 2005-3059[R]. 2005.

[23] HOKE J, BRADLEY R, SCHAUER F. Heat transfer and thermal management in a pulsed detonation engine: AIAA 2003-6486[R]. 2003.

[24] PAXSON D E, DOUGLAS PERKINS H D. Thermal load considerations for detonative combustion-based gas turbine engines: AIAA 2004-3396 [R]. 2004.

[25] GHOSN L J, ZHU D. Thermal barrier and protective coating to improve the durability of a combustor under a pulse detonation engine environment: AIAA 2007-2070[R]. 2007.

[26] JIANG Zonglin, HAN Guilai, WANG Chun, et al. Self-organized generation of transverse waves in diverging cylindrical detonations [J]. Combustion & Flame, 2009, 156(8): 1653-1661.

[27] JIANG Zonglin, CHANG Lina, ZHANG Fan. Dynamic characteristics of spherically converging detonation waves [J]. Shock Waves, 2007, 16(3):257-267.

[28] SOLOUKHIN R I. Shock waves and detonations in gases [J]. Journal of the American Chemical Society, 1967, 89(6):1542-1542.

Mr. **Li Jianzhong** received the Ph. D. degree in Aerospace Propulsion Theory and Engineering from Nanjing University of Aeronautics and Astronautics, Nanjing, China, in 2006. From 2006 to present, he has been with the College of Energy and Power, Nanjing University of Aeronautics and Astronautics (NUAA), where he is currently an associate professor. During 2009 to 2012, he was a Postdoctoral Research Fellow in AVIC Aviation Powerplant Research Institute, Zhuzhou. During 2014 to 2015, he was a visiting scholar in Mechanical Engineering, Purdue University, West Lafayette, USA. His research has focused on combustion technology of gas turbine engine, pulse detonation engine and wave rotor.

Ms. **Yuan Li** received the master degree in Aerospace Propulsion Theory and Engineering from Nanjing University of Aeronautics and Astronautics, Nanjing, China, in 2008. From 2008 to present, she has been with the School of National Defense Engineering, PLA University of Science and Technology, where she is currently an assistant professor.

Prof. **Wang Jiahua** received B. S. degree in aero-engine from Eastern China Aeronautics Institute. His research has focused on combustion technology of gas turbine engine, pulse detonation engine.

(Executive Editor: Zhang Bei)